

Ab initio theory of magnetic interactions at surfaces

This article has been downloaded from IOPscience. Please scroll down to see the full text article.

2004 J. Phys.: Condens. Matter 16 S2557

(<http://iopscience.iop.org/0953-8984/16/26/027>)

View [the table of contents for this issue](#), or go to the [journal homepage](#) for more

Download details:

IP Address: 129.252.86.83

The article was downloaded on 27/05/2010 at 15:42

Please note that [terms and conditions apply](#).

Ab initio theory of magnetic interactions at surfaces

C Sousa¹, C de Graaf², N Lopez¹, N M Harrison^{3,4} and F Illas¹

¹ Departament de Química Física i Centre de Recerca en Química Teòrica, Universitat de Barcelona i Parc Científic de Barcelona, C/ Martí i Franquès 1, E-08028 Barcelona, Spain

² Departament de Química Física i Inorgànica, Universitat Rovira i Virgili, P. Imperial Tarraco 1, E-43005 Tarragona, Spain

³ Department of Chemistry, Imperial College of Science, Technology and Medicine, London SW7 2AY, UK

⁴ CCLRC, Daresbury Laboratory, Daresbury, Warrington WA4 4AD, UK

E-mail: Nicholas.Harrison@ic.ac.uk and f.illas@qf.ub.es

Received 4 June 2003

Published 18 June 2004

Online at stacks.iop.org/JPhysCM/16/S2557

doi:10.1088/0953-8984/16/26/027

Abstract

The low to high spin energy transition of Ni adsorbed on regular and defective sites of MgO(100) and the relative strengths of bulk and surface magnetic coupling constants of first row transition metal oxides (MnO, FeO, CoO, NiO and CuO) are taken as examples to illustrate some deficiencies of density functional theory (DFT). For these ionic systems a cluster/periodic comparison within the same computational method (either DFT or Hartree–Fock) is used to establish that embedded cluster models provide an adequate representation. The cluster model approach is then used to obtain accurate values for the magnetic properties of interest by using explicitly correlated wavefunction methods which handle the electronic open shell rigorously as spin eigenfunctions.

1. Introduction

The formulation of the Hohenberg–Kohn (HK) theorems [1] has been of fundamental importance in the application of quantum mechanics to realistic systems of practical interest. The HK theorems establish the mathematical basis of density functional theory (DFT), a mathematical and computational framework which allows one to overcome most of the difficulties encountered in attempting to solve, albeit approximately, the time-independent Schrödinger equation of a many-electron system. This is because, while the traditional approaches of quantum chemistry [2, 3] focus on finding suitable approximations of the N -electron wavefunction, DFT focuses on the electron density [4, 5], a much simpler mathematical object. In DFT one abandons the idea of obtaining approximate solutions for the ground state eigenfunction of the many-electron Hamiltonian, which defines the time-independent Schrödinger equation, and instead one exploits the possibility of obtaining the

exact ground state energy from the one-particle density provided the exact, universal, density functional is known. This approach has led Kohn and Sham [6] to propose the currently almost universally used practical and elegant implementation of DFT. The Kohn–Sham approach is based on the assumption that, for any real system, a hypothetical system of non-interacting electrons exists which has the same electron density. The energy of the system is obtained by applying the functional to this density. The hypothesis assumed by Kohn and Sham is not straightforward and has generated literally hundreds of papers dealing with the so-called V -representability and N -representability problems [7–10]. These have finally been elegantly solved by Levy’s constrained search method [11]. For any representable density, the variational HK theorem applied to the non-interacting system must then lead to the exact density and, hence, exact ground state energy of the real (non-degenerate) system.

In the Kohn–Sham formulation the electron density of the independent-electron system is written in terms of single Slater determinants [6]. In this way one ensures that the wavefunction of the non-interacting N electrons fulfils the Pauli exclusion principle. The single determinant nature of the Kohn–Sham formalism allows DFT to be applied to atoms, molecules, surfaces and solids [7–10, 12–15], but it is in the two latter applications where it has generated a genuine revolution, opening up a new field of research devoted to the first-principles study of materials. In addition, the non-local character of the potential appearing in the Kohn–Sham equations leads to a formal $O(N^3)$ scaling of the problem with respect to the number of particles in the system as opposed to $O(N^4)$ in the Hartree–Fock (HF) method or $O(N^6)$ and higher in the explicitly correlated methods [2, 3]. More recently DFT has been implemented using $O(N)$ algorithms [16], where the cost of the calculation scales linearly with the number of particles in the system [17–21].

From the preceding short discussion about DFT it appears that the formalism provides a robust and accurate approach for computing the ground state energetics of almost all possible systems. However, a deeper analysis of the Kohn–Sham formalism reveals that some weak points still exist when attempting to apply DFT to open-shell systems. In fact, the key quantity in the HK theorems is the electron density and hence there is no explicit dependence on spin properties. For closed-shell molecules and non-magnetic solids this poses no problem because in any case the total spin is zero. For most atoms, open-shell molecules and magnetic solids the correct treatment of spin is essential for describing the ground state energetics and a number of observables. To address this problem a spin polarized version of DFT was proposed which is similar to the well-known unrestricted HF method [2] and which suffers from similar deficiencies. Spin polarized DFT uses a Kohn–Sham determinant with different orbitals for different spins. The formalism is motivated by determining the dependence of the total energy on the charge and spin densities, where the spin density is defined as the expectation value of S_z . Consequently, the square of the total spin operator, S^2 , is not well defined and is usually evaluated as an expectation value of the Kohn–Sham orbitals. This poor definition of S^2 is a direct result of the fact that only one-electron operators have a precise meaning in DFT and the square of the total spin is an N -electron operator. There is, of course, a functional of the charge and spin densities which will yield S^2 but the form of this functional is not known and the expectation value usually implemented is unlikely to be a good approximation to it. The Kohn–Sham determinant in DFT is not an approximation to the wavefunction; it is only a convenient way of representing the ground state electron density. Nevertheless, if one assumes that computing the expectation value of the total spin operator is valid in DFT one observes that often spin polarized solutions suffer from what in UHF theory would be called ‘spin contamination’. More importantly there are cases where it appears that the correct spin symmetry of the electronic ground state cannot be properly represented by a single determinant. This is obvious for the low spin states of atomic multiplets but it does

also appear in the open-shell singlet states characteristic of biradicals and of antiferromagnetic systems [22, 23]. In these and other cases it is hard to see how the multireference character of the electronic wavefunction can be captured by the Kohn–Sham formalism [24, 25]. In these cases, although it is clear that an energy functional which corrects for the deficiencies in the structure of the Kohn–Sham single determinant must exist, it is also clear that this would be extremely complicated and is not well represented by functionals in current use.

Clearly a rigorous description of the magnetic problems in surfaces and solids requires a different strategy. In this work we will show that there is a class of materials for which a combined use of periodic and cluster models together to a combined use of DFT and the wavefunction methods of molecular quantum chemistry leads to a rigorous description of magnetic properties either for the bulk or for the surface.

2. Open-shell states in density functional theory

The problems encountered in the description of open-shell systems commented on in the previous section, although too often ignored, are well known. They have been long known and several remedies have been proposed, including a formulation of DFT including the constraints to give the correct values of the spin operators [26]. The first attempt to compute singlet–triplet splitting through the $X\alpha$ -scattered wave method, a primitive version of DFT including Slater exchange but ignoring the correlation functional, was reported about 30 years ago by Bagus and Bennett [27]. Later on, Ziegler *et al* [28] proposed a similar approach, called the sum rule, to approach the energy of the atomic multiplets. In this approach one starts by constructing a configuration state function and hence the total square spin operator and the total z component are well defined. Similarly, Noodleman *et al* [29–31] proposed the broken symmetry approach to study open-shell singlets in antiferromagnetic systems. This approach was also initially used in the framework of the $X\alpha$ method and later Yamaguchi *et al* [32–34] used it in connection with the UHF method. In the broken symmetry approach one does not attempt to construct a spin eigenfunction but to directly compute the energy approach of the open-shell singlet from a suitable mapping [23, 35, 36]. The sum rule has only occasionally been used whereas the broken symmetry approach is widely used in the study of magnetic systems (see [22, 23] and references therein). The problem of describing atomic multiplets by current DFT methods has also been described rather recently [37].

Up to this point we have briefly described the essential features of DFT and pointed out the formal problems of the current Kohn–Sham implementation when trying to tackle open-shell systems. Another important issue concerns the practical implementation: this is the form chosen to approximate the universal exchange correlation functional. A tremendous step towards the practical implementation of DFT was given by Vosko *et al* [38] who were able to use essentially exact solutions of the Schrödinger equation for the homogenous electron gas and from this to propose a form for the correlation functional. This functional, together with the Slater formula for the exchange energy of the one-electron density, provides the local density approximation (LDA) to DFT. LDA has been shown to provide accurate molecular geometries and vibrational frequencies but its use in chemistry has been somewhat limited because of the general trend to overestimate binding energies [39]. However, LDA has been extremely important in solid state physics as it provides an *ab initio* determination of the band structure only previously available from semi-empirical tight binding theory [13]. However, the shortcomings of LDA also appear in condensed matter calculations; LDA fails to predict the proper electronic ground state of many narrow band systems [40–45]. Further refinements to the exchange–correlation functional, like the generalized gradient approximation (GGA) [46, 47], do not fully repair the artefacts introduced by the LDA [48].

NiO, and other ionic systems with localized d open shells, are predicted to be metals by the LDA and to be either metallic or to have much too small a bandgap by the GGA and thus an erroneous metallic or semiconducting behaviour is predicted [49–51]. Other improvements of LDA involve adding an effective on-site repulsion: the resulting method is usually referred to as LDA + U [52, 53]. This approximation improves the gap and the lattice constant but it involves the introduction of two, system-dependent, semi-empirical parameters [53]. A different and sophisticated post-LDA method is the so-called GW approximation. This technique aims at repairing the self-energy correction in a formally acceptable way and successfully introduces a gap in NiO, which in the self-consistent implementation of the theory is ~ 3.7 eV [54], in excellent agreement with experiment. It is interesting to note that the self-consistency condition is important, as the earlier non-self-consistent implementation of the theory gives a gap of ~ 5.5 eV which is significantly larger than experiment [55]. The GW approximation also improves the magnetic moments and density of states relative to the LDA.

The DFT methods described in the preceding paragraph all start from LDA and attempt to repair the tendency of LDA to excessively delocalize the electron density [56] which results in its underestimation of the bandgap. An alternative approach is to choose a different starting point. In this respect, the HF method either for closed-shell systems or in its spin polarized (or spin unrestricted) implementation provides a suitable zeroth-order approximation which is, in principle, equally good for molecular systems or for surfaces and solids. Moreover, periodic UHF properly describes the insulating character of this class of materials [57–63] where LDA fails. Nevertheless, the UHF method considerably overestimates the bandgap. The fundamental reason for this deficiency in the UHF method is the neglect of electron correlation. For molecular systems the effects of electronic correlation can be systematically included by means of the configuration interaction expansion of the N -electron wavefunction [2]. Unfortunately, for extended systems, this approach cannot be used in general although substantial progress has been made in the last few years [64–66]. At first sight a logical way to improve the UHF description is to use exact Fock exchange in conjunction with a correlation functional as suggested by various authors [67, 68]. Unfortunately, this approach does not significantly improve the description of the bandgap [51]. Very significant progress has been made through the introduction of hybrid exchange density functionals [69–71] in which the exact Fock exchange is mixed with a given exchange functional while the correlation is treated within the density functional framework. A particularly successful combination of exchange and correlation functional is the so-called B3LYP method [70] which uses three parameters to achieve the best fit to experimental thermochemical data of a series of molecules and combines the exact Fock exchange with the gradient corrected exchange functional proposed by Becke [69], and with the non-local expression of the correlation functional proposed by Lee *et al* [72], based on the original work of Colle and Salvetti [67, 68]. These functionals appear to be very well suited to describe not only the bandgap [51, 73–76] but also the magnetic coupling constants [36, 74, 77] of these insulating ionic systems.

The numerical performance of the hybrid functionals is significantly better than GGA functionals but the fundamental problem regarding the total spin remains. This problem has direct consequences for the evaluation of properties of molecules, surfaces and solids such as the interpretation of electron paramagnetic resonance spectra [25], the magnetic coupling parameters either in biradicals, dinuclear complexes, surfaces and solids [22, 23] and the adsorption energy of transition metal atoms [78, 79]. A particular example of the failure of DFT methods in the study of surface phenomena is the chemisorption of NO on NiO(100) and on Ni-doped MgO(100) [24, 25]; this point is discussed further in another paper of this special issue. Fortunately, the magnetic ionic solids and surfaces where DFT encounters most of the severe problems can be adequately represented by cluster models. This is an important

feature because cluster models can be studied using the most sophisticated explicitly correlated wavefunction methods. This allows one to study the performance of current and new exchange–correlation functionals and thus provide a definitive test of the validity of a given approach. In this work we focus on the performance of DFT in two well defined problems; the excitation energy of Ni atoms adsorbed on regular and O-vacancy sites of the MgO(100) surface and the magnetic coupling between surface magnetic ions of several transition metal oxides. To this end accurate, explicitly correlated, wavefunction methods are used in embedded cluster models and the results compared to those obtained from different DFT schemes. Simultaneously, cluster models for these systems are validated by comparing results for the property of interest to those obtained using a periodic approach and the same DFT method. This strategy allows a definite and precise statement on the performance of a given DFT approach for a given problem involving open shells to be made and is thus of great help in assessing the quality of a given DFT calculation on a particular system and also in attempting to improve the present exchange–correlation functionals.

3. The embedded cluster model approach

This section describes the strategy used to construct an accurate representation of an ionic crystal from a local point of view. We will illustrate each step with the two examples chosen in this work: the modelling of Ni adsorption on different sites of the MgO surface [78, 79] and the construction of a cluster model to investigate the magnetic coupling between two spin moments localized on the nickel ions in bulk and surface NiO [80, 81]. A similar discussion about the modelling of ionic oxide surfaces has been reported recently [82].

3.1. Quantum cluster region

The first step in the construction of an adequate embedded cluster model is to identify the local part of the systems one wishes to represent, the rest of the crystal defining an ‘outer’ region. The local region is to be treated with highly accurate quantum chemical computational schemes whereas the outer region is designed to provide an appropriate representation of the rest of the system and is treated in a more approximate way. The local region necessarily includes the atoms that play a fundamental role in the property under study and its choice will always be a balance between precision and feasibility. In the case of Ni adsorption on MgO(100) we consider adsorption at a regular O-site and at an O-vacancy. For the former the local region contains an O-centred stoichiometric $O_{13}Mg_{13}$ cluster (figure 1(a)) whereas in the later the local region is the same except for the removal of the central O atom (figure 1(b)). For the magnetic coupling problem, our second example, at least two magnetic centres (Ni^{2+} ions) and the bridging ligand in between them, i.e. a Ni_2O cluster, have to be included. However, previous cluster model studies have shown that the complete oxygen coordination shell of each nickel must be added to the local region, which gives rise to a Ni_2O_{11} cluster to represent bulk NiO and to a Ni_2O_9 model to study magnetic coupling between surface atoms. As a general rule, the local quantum region contains the atoms directly involved in the property under study and the first shell of atoms around those centres. It is important to remark that in some cases, for instance when large relaxations are predicted by geometry optimizations, such a local region is not sufficient and a larger number of atoms has to be considered explicitly in this region.

3.2. Static short-range interactions

The embedding of the local region of the cluster model must account for the short-range electrostatic repulsion between the cluster atoms and those surrounding them. Since this

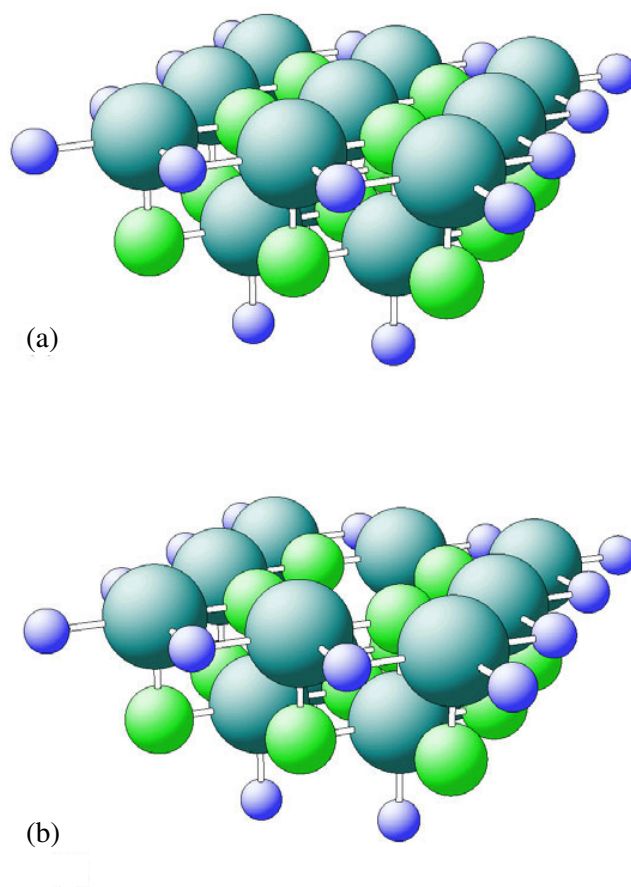


Figure 1. Cluster model describing the regular surface and the oxygen vacancy. (a) $[\text{O}_{13}\text{Mg}_{13}] + \text{TIPs}$ and (b) $[\text{O}_{12}\text{Mg}_{13}] + \text{TIPs}$. Small spheres represent TIPs, medium spheres Mg cations and large spheres O anions.

(This figure is in colour only in the electronic version)

is a quantum mechanical effect simple embedding schemes based on classical models cannot be employed and more elaborate schemes have to be invoked. Several different approaches have been developed over the years, but we will only mention here the total ion potential (TIP) [83, 84] embedding and the more rigorous *ab initio* embedding model potential (AIEMP) scheme [85, 86]. In both methods the interaction of the cluster electrons with those in the outer region is effectively taken into account through an effective one-electron operator acting on the electrons of the atoms in the local region only. This is a computationally efficient procedure and its use is straightforward, especially if some of the ions external to the cluster are represented by effective core TIP potentials [83]. This method is, however, restricted to cations only, since sufficiently large core pseudopotentials cannot be constructed for anions such as O^{2-} . In our example of constructing a cluster model for bulk NiO, the coordination of each oxygen atom in the Ni_2O_{11} quantum cluster region is completed with Ni^{2+} TIPs to avoid the artificial delocalization of the oxygen atoms in the cluster. This results

in a $\text{Ni}_2\text{O}_{11}\text{Ni}_{28}$ embedded cluster, where the latter 28 Ni^{2+} ions are represented by TIPs. A similar procedure is used to embed the $\text{O}_{13}\text{Mg}_{13}$ surface cluster model (figure 1(a)) for $\text{MgO}(100)$, the corresponding model with the oxygen vacancy (figure 1(b)) or for the Ni_2O_9 surface cluster model of NiO . The general rule is to include the first-neighbour shell of cations surrounding each anion in the local region.

3.3. Long-range electrostatic interactions

In the present examples long-range interactions arise from the electric field generated by all ions in the crystal and are easily incorporated in the model by calculating the Madelung field of the ions not included in the cluster and adding this potential to the cluster Hamiltonian. For this purpose, first the exact Madelung field is calculated by an Ewald summation with formal point charges at the lattice positions. From this total potential the contribution of the cluster ions is subtracted. The use of formal charges is consistent with the assignment of an integer number of electrons to the cluster. There are essentially three methods to include the effects of the resulting Madelung field. The first one is the Evjen method [87] which consists in setting the value of the point charges at the lattice positions in the cluster edge and far from the local region according to the restriction of overall charge neutrality. This restriction often results in a fast convergence of the Madelung potential with the number of point charges included in the outer region. The overall charge neutrality is achieved by setting formal charges at all lattice positions except for the charges in the outermost shell. For a cubic lattice half of the formal charge is used for the faces; a quarter for the edges and one eighth for the vertices. The method is, however, not applicable for any type of crystal and does not give accurate representations of the Madelung field except for the simplest lattices like fcc [88]. A more general scheme is fitting a small set of point charges at lattice positions within a certain radius around the cluster to the exact value of the potential at a large number of points in a grid around the cluster local region [88]. Finally, we mention a third approach in which all charges within a sphere of radius r around the centre of the cluster are taken [89]. The radius is, however, taken such that the overall charge of all centres within the sphere is zero in order to ensure a good convergence of the resulting potential. For the examples included in the present work, these three methods are equally valid.

For the case of Ni on MgO an array of $16 \times 16 \times 4$ point charges with formal ± 2 values has been used. In this case, the use of a stoichiometric cluster and the high ionicity of MgO enables one to avoid the use of a more sophisticated approach. For the Ni_2O_{11} and Ni_2O_9 clusters a small set of point charges have been optimized to reproduce the Madelung potential.

3.4. Long-range polarization

The response of the crystal to changes in the electronic structure of the quantum cluster region is more difficult to account for than the static interactions discussed in the previous subsection. An *ab initio* scheme to include this effect has been described by Barandiarán and Seijo [90]. An even more rigorous treatment to account for the long-range polarization has been developed by Pisani and co-workers [91, 92]. However, these methods are far from being routine and are also computationally demanding. Consequently, other simplified methods are used. Here we mention those based on the classical Born formula [93] and the so-called shell model method [94, 95].

The long-range polarization is, however, only important when charges are created in the quantum cluster region and this is not the case for the examples included in the present work.

4. The periodic approach

A perfect crystal surface or bulk solid can be imagined as the repetition of a motif usually referred to as a unit cell. The use of this translational symmetry in electronic structure calculations allows the periodic system to be modelled without the somewhat arbitrary partition discussed in the previous section. Periodic calculations are nowadays almost routine and several efficient computer codes exist [96–102]. In all cases the electron density is represented by means of a Slater determinant and the orbitals (HF or KS) obtained by a self-consistent-field procedure at a series of points in the reciprocal space. Consequently, the periodic calculations suffer from the problems described in the introduction when dealing with magnetic systems. However, they have the advantage of describing an extended system and thus of treating all long-range fields correctly. Nevertheless, one must caution that there are situations where the periodic approach may not be easily used. This is the case of point defects which are often present in very low concentrations. Very large supercells are required to describe these particular systems and even in this case it may well be that cluster and periodic models are equally far from the real systems one wishes to describe.

In the present work periodic calculations will be used for a few cases mainly to validate the cluster approach outlined above. Further details concerning this type of calculation will be given when discussing the particular examples.

5. Computational methods

The singlet–triplet excitation energy of Ni adsorbed on the O- and the O-vacancy sites of MgO(100) has been studied using DFT and wavefunction based methods. For the former the Perdew–Wang GGA [46, 47] and hybrid B3LYP [70] methods were chosen whereas for the second we use the complete active space self-consistent field (CASSCF) and the second-order perturbation theory (CASPT2) methods. In the CASSCF method one starts defining a number of active electrons and active orbitals and a full configuration interaction wavefunction is obtained by distributing all active electrons in all active orbitals in all possible ways. The orbitals and configuration interaction expansion coefficients are solved variationally [103–105]. CASSCF is very well suited for multiconfigurational problems but it does not include the so-called dynamical electron correlation effects. To include these effects second-order perturbation theory calculations are carried out using the CASSCF wavefunction as the zeroth-order approximation. The resulting method is usually referred to as CASPT2 [106, 107]. For the GGA and B3LYP calculations a contracted Gaussian basis set has been used to describe the electron density. The basis for the Mg atoms close to the central oxygen (or vacancy) is [13s8p/6s3p] whereas a smaller [12s7p/5s2p] set is employed for the remaining Mg atoms. For O atoms the basis set employed is of double- ζ quality [8s4p/4s2p], the s and p primitives having been optimized to describe the O⁻ anion. An extra polarization d function was added to the central O atom of the regular surface cluster model. Finally, for Ni the uncontracted basis set and pseudopotential reported by Hay and Wadt [108] have been used; further details can be found in previous work [78, 79]. For the CASSCF/CASPT2 two different basis sets have been used, the first one (basis 1) is the same used in the cluster DFT calculations and is used mainly for comparison. The second set (basis 2) uses the generally contracted atomic natural orbital (ANO) basis sets [109–112] and is (6s, 5p, 4d, 1f) for Ni, (4s, 3p, 1d) for central O, (4s, 3p) for the five Mg atoms closest to the central oxygen site and (3s, 2p) for the other eight cations in the third coordination sphere, and (3s, 2p) for the remaining 12 oxygen atoms. The active space contains the Ni 3d and 4s orbitals plus a set of

virtual d orbitals leading to a CAS with 10 electrons and 11 orbitals. For the interaction of Ni on the regular O-site only the perpendicular distance of the metal atom to the surface has been optimized either at the B3LYP or CASSCF levels of theory. For the interaction above the oxygen vacancy the four Mg atoms closest to the vacancy have also been allowed to relax. The cluster CASSCF/CASPT2 calculations have been carried out using the MOLCAS [105] package, while the Gaussian98 suite of computer programs has been used to carry out the GGA and B3LYP cluster calculations. Slab periodic calculations carried out at the GGA level will also be reported mainly for comparison purposes. A cutoff energy of 25 Ryd and ultrasoft pseudopotentials [113] have been used. Both the regular surface and the neutral oxygen vacancy (coverage 0.25 ML) have been studied for the adsorption of a single atom and monolayer. For these models a Monkhorst–Pack $[4 \times 4 \times 1]$ mesh has been employed and changed accordingly for smaller unit cell calculations. The slab contains 3 atomic layers and unit cell parameters are those employed for the cluster calculations with more than 10 Å between the repeated slabs. A correction for the electric field in the vacuum region has been employed. For the vacancy a $p(2 \times 2)$ unit cell was used. Atoms in the first layer have been relaxed and, in all cases, the z component of the adsorbate. The periodic calculations have been carried out using the plane-wave pseudopotential DACAPO computer code [102].

The energies necessary to compute the bulk and surface magnetic coupling constants of various transition metal oxides (MnO, FeO, CoO, NiO and CuO) have been computed using CASSCF/CASPT2 on suitable embedded cluster models and using large ANO basis sets. For the transition metal the ANO basis set [109, 112] is (6s, 5p, 3d, 1f), the oxygen atom bridging the two metals is described by a (5s, 4p, 1d) ANO set whereas a smaller (4s, 3p) is used for the remaining oxygen atoms in the cluster. In all cases the active space contains the open-shell orbitals and electrons. Thus for MnO, FeO and CoO, the active space contains the 3d atomic orbitals of each transition metal atom and the corresponding number of d electrons is 10, 12 and 14, respectively. For NiO and CuO it is necessary to use an extended space [114] which leads to a CAS with 6 and 8 electrons in 10 orbitals for NiO and CuO, respectively. The 3s, 3p and 3d electrons of the transition metal atoms and the 2s and 2p electrons of oxygen have been explicitly correlated in the CASPT2 calculations. Some comments concerning a comparison between cluster and periodic calculations at the UHF and B3LYP levels of theory will be introduced for comparison.

6. Low and high spin states of Ni adsorbed on MgO(001) regular O- and O-vacancy sites

The Ni atom is quite a special case for DFT because the relative energies of the multiplets corresponding to the lowest electronic configurations are strongly dependent on the computational method used. From experiment it is known that the nickel-atom lowest states are triplet states, the electronic ground state, including spin–orbit effects, being the 3F_4 level from the d^8s^2 configuration which is only 0.025 eV below the 3D_3 level of the d^9s^1 manifold [115]. The weighted average of the 3F and 3D multiplets gives the opposite order with an energy difference which is only 0.011 eV in favour of the $^3D(d^9s^1)$. The singlet 1S_0 level from the d^{10} configuration is 1.826 eV above the 3F_4 . In a previous work [78] it has been shown that HF (either spin restricted or unrestricted) gives too large an energy difference between the two triplet configurations. Both predict the d^8s^2 configuration as the ground state with the d^9s^1 configuration lying 1.27 eV (HF limit) or 1.46 eV above the d^8s^2 HF energy. Explicit introduction of electronic correlation by multireference configuration interaction methods drastically changes the order of stability and, as expected, correctly predicts that d^9s^1 and d^8s^2 are nearly degenerate in agreement with experiment [116, 117]. However, DFT produces

Table 1. Vertical distance (in Å) of Ni to the regular (O site) and vacancy (F_S site) sites of the MgO(100) surface. For the F_S site the position of the Mg cation as nearest neighbour to the vacancy has been relaxed.

Method/model	Low spin state		High spin state	
	z^\perp (O site)	z^\perp (F_S site)	z^\perp (O site)	z^\perp (F_S site)
GGA/slab	1.82	1.46	1.98	1.85
GGA/cluster	1.81	1.45	2.03	1.87
B3LYP/cluster	1.82	1.44	2.12	1.93
CASPT2 ^a /cluster	1.88	1.38	2.07	1.75

^a Basis 2.

very different results, depending on the choice of the exchange–correlation functional, the exchange term having a drastic effect. Thus, GGA gives too large a correction of the inter-configuration energy [118]. The d^8s^2 configuration appears to have an excessively high energy and as a result the d^9s^1 configuration energy lies 3.74 eV below the former which, one must recall, is the experimental ground state. This is an important point because the atomic reference energy is an important component of periodic DFT calculations. In contrast to the pure DFT methods the hybrid approaches perform surprisingly well, the B3LYP results being very close to the experimental data [79].

The electronic state of Ni with the oxygen regular and defective sites of MgO(100) is the result of a balance between the tendency of Hund’s rule to preserve the atomic state and chemical covalent terms tending to form chemical bonds and hence to quench the atomic magnetic moment [78]. Hence, the stronger the interaction the smaller the difference between the high and low spin states. The fact that the interaction of Ni with a surface oxygen vacancy (i.e. a surface F centre— F_S) is stronger than for a regular site [119–121] implies that the high to low spin state energy transition should be expected for the latter and this is precisely the conclusion of a recent DFT study [79]. However, for a regular site the result is not so predictable, mainly because of the strong dependence of the adhesion energy on the choice of the DFT method [122, 123]. Clearly, there is a further need to validate the DFT results, especially with respect to the total spin of the electronic ground state and the high to low spin energy transition. To this end CASPT2 calculations have been carried out for the interaction of Ni with a regular O site of MgO and with an oxygen vacancy: the F_S centre.

The vertical distance from Ni to the regular and defective sites of MgO(100) is reported in table 1 for different models and methods. Several important points emerge from the summary of results in table 1. First of all, it is important to see that all methods and models predict the same qualitative trends. Thus all methods and models predict, for both surface sites, a longer distance for the high spin state and also significantly smaller distances when the interaction takes place above the F_S centre. Secondly, it is worth pointing out that at the GGA level the differences between slab and cluster are almost negligible for the low spin state (~ 0.01 Å) and moderately small (~ 0.05 Å) for the high spin state. This result supports the use of embedded cluster models for the subsequent analysis. The next important point is the relatively small effect of the exchange correlation functional in determining the equilibrium distance of the metal atom above the surface. Fourth, the difference between B3LYP and CASPT2 is of the order of 0.05 Å except for the high spin state when the interaction occurs above the F_S site. This larger difference is probably due to the fact that the optimization of the O-vacancy five-nearest-neighbour cations has been carried out at the CASSCF only. Overall we can conclude that the uncertainty in the determination of the equilibrium distance is smaller than 0.05 Å.

Table 2. Low to high spin adiabatic energy transition (Δ_{L-H} in electronvolts) for Ni adsorbed on the regular (O site) and vacancy (F_S site) sites of the MgO(100) surface. A negative value means that the high spin state is more stable than the low spin state.

Method/model	Δ_{L-H}	
	O site	F_S site
GGA/cluster	0.30	0.90
B3LYP/cluster	-0.03	0.38
CASSCF ^a /cluster	-0.06	-0.32
CASPT2 ^a /cluster	0.41	0.87

^a Basis 2.

Next we consider the adiabatic low to high spin (or singlet–triplet) energy transition (Δ_{L-H}); this is the smallest possible energy difference between the two electronic states because it is computed by the difference of the total energies at the minimum of the potential energy curve. This is a more delicate quantity and we show below that it is very sensitive to the computational method. We have already argued that GGA fails to reproduce the energy difference of the lowest electronic configurations of the Ni atom. Consequently one expects a similar behaviour in the description of the low to high spin energy difference of Ni adsorbed on MgO(100). Results in table 2 show that this is not the case, the GGA results being very close to those predicted by the more accurate CASPT2 approach. However, this behaviour is also the consequence of the general GGA tendency to overestimate the adsorption energy [124] which in this case favours the low spin state [78, 79]. Table 2 shows also that the B3LYP predictions are almost qualitatively correct although at this level the high and low spin states are found to be almost degenerate. This contrasts with the CASPT2 calculations that predict for the regular site the singlet state to be 0.41 eV lower than triplet. This difference is even larger (0.87 eV) for the interaction above the F_S centre as expected from the stronger interaction on this site but only 0.38 eV according to the B3LYP. A point deserving further comment is the dominant role of dynamical electronic correlation in determining the final value of the value. Notice that the CASSCF, which does not include dynamical correlation effects, predicts a qualitatively wrong behaviour predicting a triplet state ground state. This wrong prediction of the CASSCF method can be easily explained as the result of competition between the need to preserve the atomic ground state of the transition metal atom (Hund’s rule) and the effects of covalent bonding; the latter are underestimated at the CASSCF level and this results in a triplet ground state. At this point the B3LYP result is quite notable although the values are underestimated by ~ 0.5 eV.

From this example several conclusions can be drawn. First, embedded cluster models provide adequate representation of ionic surfaces and can be used to study the nature of the metal support interaction. Second, DFT and wavefunction methods are both able to describe the equilibrium geometry of adsorbed transition metal atoms on an ionic surface such as Mg(001). Finally, a low spin character of the interaction of Ni on the regular surface sites of MgO is predicted by the CASPT2 method, while the B3LYP predicts a near-degeneracy of low and high spin states. Notice that the correct answer predicted by GGA is fortuitous and arises from the overestimate of the interaction energy [78, 79]. In the case of the interaction above a F_S centre all methods (GGA, B3LYP and CASPT2) predict a low spin state, as expected from the stronger interaction. The fact that B3LYP is able to almost reproduce the low spin nature of the interaction of Ni on MgO(100) is quite remarkable since the analysis of the CASSCF reference wavefunction shows that, in the lowest singlet, Ni has an effective d^9s^1 electronic configuration.

7. Surface versus bulk magnetic coupling in first row transition metal oxides

In the previous section it has been established that embedded cluster models provide an adequate representation of ionic surfaces. For systems involving transition metal atoms with unfilled d shells similar results are found when considering the energy difference corresponding to the low and high spin states that can be constructed by antiferro- or ferromagnetic coupling of the effective spin in each centre. In fact, a detailed comparison of cluster or periodic HF for a variety of systems such as KNiF_3 and K_2NiF_4 [35], various high critical temperature superconductor parent compounds [125–131], NiO bulk [80, 132] and surface [81], CuF_2 [59], the SrCu_2O_3 ladder compound [133] or the Sr_2CuO_3 , Ca_2CuO_3 and Li_2CuO_2 linear chains [134, 135] has unequivocally established that the Heisenberg magnetic coupling constant is a local property which is equally well reproduced by periodic or cluster models of the corresponding materials. The locality of these interaction have also been analysed in terms of effective Hamiltonian theory [136].

From the discussion above it turns out that, for a given ionic magnetic material, it is possible to predict the magnitude of the various magnetic coupling constants using suitably embedded cluster models. This is an important point because it has also been shown that the actual value of the magnetic coupling constants predicted from DFT methods exhibits a large dependence on the choice of the exchange–correlation functional [36, 77]. The cluster model allows one to compute the magnetic coupling constant using explicitly correlated wavefunction methods. In this section we will focus on the surface and bulk magnetic coupling constant of transition metal oxides as predicted from CASPT2 calculations. It has been demonstrated that this approach provides a reasonable estimate of this delicate property which, for the present purposes, is sufficiently accurate [114]. More accurate results, in extremely good agreement with experiment [128, 137], can be obtained by making use of the so-called difference dedicated configuration interaction method described elsewhere [138, 139].

In this section we report the results of CASSCF/CASPT2 calculations on the magnetic interactions in the series of late transition metal oxides (TMO) ($\text{TM} = \text{Cu, Ni, Co, Fe, Mn}$) by focusing on the difference between the surface and the bulk values for the magnetic coupling constant. The motivation for comparing bulk and surface coupling comes from a previous study where it was shown that the surface magnetic coupling constant J is significantly smaller than that in the bulk [81]. It has been shown that the decrease of J is completely determined by the lower coordination of the Ni ions at the surface and that the lower Madelung potential at the surface only has a minor influence on the magnetic coupling. Similar results have been found from periodic UHF [140] and hybrid DFT calculations [141]. This result is, however, in contrast to another theoretical prediction based on the Hubbard model Hamiltonian, which predicts an increase of the coupling at the surface of $\sim 50\%$ [142]. Recently, a helium atom diffraction study of the antiferromagnetic transition on the NiO(100) surface has been published. The interpretation of the experimental data suggests that the magnetic coupling at the surface is lower than in the bulk [143, 144]. Therefore it is interesting to compare the trend along the series and to verify whether the decrease in J predicted for NiO is a general phenomenon.

In principle one expects that the magnetic interaction in this series decreases from Cu to Mn, since the decrease of the nuclear charge on the metal causes an increase in the charge transfer energy and, hence, a decrease in the importance of the covalent interactions. To facilitate the comparison between the different compounds, we use idealized structures for CuO and FeO, whose real crystal structure show defects and/or orthorhombic distortions. The lattice parameters are as follows: 4.087 and 4.332 Å for CuO and FeO (an extrapolation to $x = 0$ of FeO_{1-x}), respectively. Those for the other compounds are taken from the crystallographic

Table 3. Magnetic coupling constants (in millielectronvolts) for bulk and surface transition metal oxides as predicted from embedded cluster model CASPT2 calculations. The M–O oxide (in bohrs) is also given for completeness.

	MnO	FeO	CoO	NiO	CuO
J (bulk)	−1.20	−2.59	−5.98	−17.3	−85.6
J (surface)	−1.12	−2.43	−5.55	−14.0	−60.4
Decrease (%)	7.1	6.6	7.2	19	29
d (TM–O)	4.190	4.093	4.025	3.930	3.862

data [145]. The metal–oxygen distances used to construct the models are given in table 3 which also contains a summary of the most important results.

Before commenting on the results for magnetic coupling it is important to point out that CoO has a degenerate ground state and hence spin–orbit effects cannot be omitted in principle. These effects have been studied in detail by Fink and Staemmler [146] both for the bulk and the 100 surface. These authors have used complete active space configuration interaction wavefunctions and conclude that the average of the two anisotropic J values calculated with the inclusion of spin–orbit interactions give exactly the present CASSCF value. Consequently, spin–orbit effects have not been included for CoO. From table 3 one first observes that the trend of decreasing magnetic interaction strength from CuO to MnO is reproduced both by CASSCF and CASPT2. Notice that the J values reported in table 3 have been obtained defining the Heisenberg–Hamiltonian as usually

$$\hat{H}^{\text{Heisenberg}} = -J \hat{S}_1 \hat{S}_2 \quad (1)$$

where J is the magnetic coupling constant and \hat{S}_1 , \hat{S}_2 are the corresponding spin operators for magnetic centres 1 and 2, using simple mapping arguments to compute J from *ab initio* energy differences [23, 35] and ensuring that the forthcoming comparison to experiment is carried out using the same definition of the model Hamiltonian. The analysis of the one-electron functions and the multireference N -electron wavefunction indicates that indeed the covalent interaction—appearing either through a mixing in the one-electron functions of the O-2p and TM-3d atomic orbitals or as configurations connected to charge transfer excitations in the N -electron wavefunction—is strongest for CuO and a gradual decrease is observed towards MnO. Secondly, the results in table 3 show that, as is well known (see [136] and references therein), the treatment of external electron correlation increases the calculated J by a factor of ~ 4 . This has been observed before in many applications and illustrates once more the necessity of accounting for this electron correlation in order to obtain reasonable estimates of the magnetic coupling parameter. The value obtained for NiO (bulk), -17.3 meV, compares very well with the experimental values of -19.8 and -17.0 meV obtained from different techniques [147, 148]. The comparison of the computed magnetic coupling constant for bulk MnO, -1.20 eV, is also in excellent agreement with the experimental value of -1.7 meV obtained from inelastic neutron scattering [149] and analysis of thermodynamic data [150]. Finally, the comparison of bulk and surface reveals the decrease, already predicted for NiO, of the magnetic interaction with the coordination number of the TM ion. However, the reduction in J is not uniform; it varies from 30% for CuO, to 20% in NiO and to roughly 7% for CoO, FeO and MnO indicating that, although this reduction is general, it depends on the particular system. This may be of importance in the study of thin film of magnetic oxides supported on various substrates.

Before concluding this section it is worth commenting that Ködderitzsch *et al* [151] describe a method to extract magnetic coupling constants at the NiO(100) surface. Their

computational method, LDA + SIC, predicts values of -12.0 and -9.5 meV for bulk and surface, respectively, both in fair agreement with the CASSCF results although still far from the experimental results which are nicely reproduced by the CASPT2 cluster model calculations.

8. Concluding remarks

In this paper we have focused in the problems encountered when applying DFT methods to open-shell systems with particular emphasis on the consequences on the description of magnetic properties. For ionic systems with unfilled d shells the resulting open-shell electrons are localized and hence it is possible to model these systems by means of embedded cluster models. The use of periodic and embedded cluster models together with unrestricted HF or any pure or hybrid DFT methods allows one to establish the validity of a given embedded cluster model because for many local properties both approaches have to provide exactly the same answer. Once a given cluster model has been validated it is possible to obtain accurate results by making use of explicitly correlated wavefunction methods. This is important because, on the one hand, it allows one to go beyond the limits imposed by the current implementations of DFT and, on the other hand, it provides useful benchmarks which should be taken into account in the development of new exchange–correlation functionals.

The strategy outlined above has been applied to two prototypical examples of magnetic interactions at surfaces. These concern the electronic ground state and high to low spin state transition for Ni adsorbed on MgO(100) and the relative magnitude of the magnetic coupling constant of bulk and surface transition metal oxides including MnO, FeO, CoO, NiO and CuO. A detailed comparison of various DFT and wavefunction methods has established the fact that DFT results have to be handled with extreme care. In fact, the GGA method fails to describe the energy differences of the low lying electronic configurations of Ni properly and predicts a low spin state whereas the B3LYP method, which performs much better in describing the atomic energies, predicts a near-degeneracy between low and high spin states. Moreover, the correct description by GGA of the spin state, is seen to be a consequence of a deficiency of the method, namely the significant overestimation of adhesion energies. For the magnetic coupling problem it is a well established fact that the magnitude of the magnetic coupling constant strongly depends on the particular choice of the exchange–correlation functional. However, a proper cluster/periodic comparison within a given DFT (or HF) approach allows one to establish the adequacy of a given embedded cluster model to be used in subsequent calculations using powerful explicitly correlated wavefunction methods.

To summarize, further development of DFT is required before this theory can be safely and routinely applied to magnetic problems in strongly correlated systems. In this sense the use of embedded cluster models is of importance since it allows appropriate wavefunction methods to be used which provide benchmarks for the subsequent improvement of exchange–correlation functionals.

Acknowledgments

This research has been supported by the Spanish MCyT grants BQU2002-04029-C02-01 and-02 and, in part, by Generalitat de Catalunya grant 2001SGR-00043. Part of the computer time was provided by the CIESCA and CEPBA supercomputing centers, through grants from the Fundació Catalana de la Recerca and from the Universitat de Barcelona. DACAPO periodic calculations have been carried out on the SP3 parallel machine of the CEPBA-IBM-Research-Institute of Barcelona. NMH acknowledges financial support of the European Community for

staying in Barcelona through the Improving Human Potential contract HPRI-CT-1999-00071 held by the CESCA-CEPBA.

References

- [1] Hohenberg P and Kohn W 1964 *Phys. Rev. B* **136** 864
- [2] Szabo A and Ostlund N S 1982 *Modern Quantum Chemistry: Introduction to Advanced Electronic Structure Theory* (New York: Macmillan)
- [3] Jensen F 2002 *Introduction to Computational Chemistry* (Chichester: Wiley)
- [4] McWeeny R 1992 *Methods of Molecular Quantum Mechanics* (London: Academic)
- [5] Parr R G and Yang W 1989 *Density Functional Theory of Atoms and Molecules* (London: Oxford Science)
- [6] Kohn W and Sham L 1965 *Phys. Rev. A* **140** 1133
- [7] Parr R G and Yang W 1989 *Density Functional Theory of Atoms and Molecules* (New York: Oxford University Press)
- [8] Dreizler R M and Gross E K U 1990 *Density Functional Theory: An Approach to the Quantum Many Body Problem* (Berlin: Springer)
- [9] Seminario J M and Politzer P (ed) 1995 *Modern Density Functional Theory: A Tool for Chemistry, Theoretical and Computational Chemistry* vol 2 (Amsterdam: Elsevier)
- [10] Seminario J M and Politzer P (ed) 1994 *Recent Developments and Applications of Modern Density Functional Theory, Theoretical and Computational Chemistry* vol 4 (Amsterdam: Elsevier)
- [11] Levy M 1979 *Proc. Natl Acad. Sci.* **76** 6002
- [12] Görling A, Trickey S B, Gisdakis P and Rösch N 1999 *Topics in Organometallic Chemistry* vol 4, ed J Brown and P Hofmann (Heidelberg: Springer) pp 109–65
- [13] Zangwill A 1988 *Physics at Surfaces* (Cambridge: Cambridge University Press)
- [14] Desjonquères M C and Spanjard D 1996 *Concepts in Surface Physics* (Berlin: Springer)
- [15] Fulde P 1991 *Electron Correlations in Molecules and Solids* (Berlin: Springer)
- [16] Strain M C, Scuseria G E and Frisch M J 1996 *Science* **271** 51
- [17] Millam J M and Scuseria G E 1997 *J. Chem. Phys.* **106** 5569
- [18] Guerra C F, Snijders J G, te Velde G and Baerends E J 1998 *Theor. Chem. Acc.* **99** 391
- [19] Ayala P Y and Scuseria G E 1999 *J. Chem. Phys.* **110** 3660
- [20] Bowler D R and Gillan M J 2000 *Mol. Simul.* **25** 239
- [21] Haynes P D and Payne M C 2000 *Mol. Simul.* **25** 257
- [22] Caballol R, Castell O, Illas F, Malrieu J P and Moreira I de P R 1997 *J. Phys. Chem.* **101** 7860
- [23] Illas F, Moreira I de P R, de Graaf C and Barone V 2000 *Theor. Chem. Acc.* **104** 265
- [24] Domínguez-Ariza D, Illas F, Bredow T, Di Valentin C and Pacchioni G 2003 *Mol. Phys.* **101** 241
- [25] Di Valentin C, Pacchioni G, Bredow T, Domínguez-Ariza D and Illas F 2002 *J. Chem. Phys.* **117** 2299
- [26] Savin A 1995 *Recent Advances in Density Functional methods* ed D P Chong (Singapore: World Scientific) p 129
- [27] Bagus P S and Bennet B I 1975 *Int. J. Quantum Chem.* **9** 143
- [28] Ziegler T, Rauk A and Baerends E J 1977 *Theor. Chim. Acta* **43** 261
- [29] Noodleman L 1981 *J. Chem. Phys.* **74** 5737
- [30] Noodleman L and Davidson E R 1986 *Chem. Phys.* **109** 131
- [31] Noodleman L, Peng C Y, Case D A and Mouesca J M 1995 *Coord. Chem. Rev.* **144** 199
- [32] Yamaguchi K, Fueno T, Ueyama N, Nakamura A and Ozaki M 1989 *Chem. Phys. Lett.* **164** 210
- [33] Yamaguchi K, Tsunekawa T, Toyoda Y and Fueno T 1988 *Chem. Phys. Lett.* **143** 371
- [34] Nagao H, Mitani M, Nishino M, Yoshioka Y and Yamaguchi K 1997 *Int. J. Quantum Chem.* **65** 947
- [35] Moreira I de P R and Illas F 1997 *Phys. Rev. B* **55** 4129
- [36] Illas F and Martin R 1998 *J. Chem. Phys.* **108** 2519
- [37] Baerends E J, Branchadell V and Sodupe M 1997 *Chem. Phys. Lett.* **265** 481
- [38] Vosko S H, Wilk L and Nusair M 1980 *Can. J. Phys.* **58** 1200
- [39] Koch W and Holthausen M C 2002 *A Chemist's Guide to Density Functional Theory* 2nd edn (Weinheim: Wiley-VCH)
- [40] Pickett W E 1989 *Rev. Mod. Phys.* **61** 433
- [41] Terakura K, Oguchi T, Williams A R and Klüber J 1984 *Phys. Rev. B* **30** 4734
- [42] Guo G Y and Temmerman W M 1988 *J. Phys. C: Solid State Phys.* **21** L803
- [43] Mattheiss L F 1994 *Phys. Rev. B* **49** 14050
- [44] Kasowski R V, Tsai M H and Dow J D 1990 *Phys. Rev. B* **41** 7744

- [45] Shen Z-X, List R S, Dessau D S, Wells B O, Jepsen O, Arko A J, Bartlett R, Shih C K, Parmigiani F, Huang J C and Lindberg P A P 1991 *Phys. Rev. B* **44** 3604
- [46] Perdew J P and Wang Y 1992 *Phys. Rev. B* **45** 13244
- [47] Perdew J P, Chevary J A, Vosko S H, Jackson K A, Pederson M R, Singh D J and Fiolhais C 1992 *Phys. Rev. B* **46** 6671
- [48] Sawada H, Morikawa Y, Terakura K and Hamada N 1997 *Phys. Rev. B* **56** 12154
- [49] Leung T C, Chan C T and Harmon B N 1991 *Phys. Rev. B* **44** 2923
- [50] Dufek Ph, Blaha P, Sliwko V and Schwarz K 1994 *Phys. Rev. B* **49** 10170
- [51] Bredow T and Gerson A R 2000 *Phys. Rev. B* **61** 5194
- [52] Anisimov V I, Zaanen J and Andersen O K 1991 *Phys. Rev. B* **44** 943
- [53] Anisimov V I, Solovyev I V, Korotin M A, Czyzyk M T and Sawatzky G A 1993 *Phys. Rev. B* **48** 16929
- [54] Massidda S, Continenza A, Posternal M and Baldereschi A 1997 *Phys. Rev. B* **55** 13494
- [55] Aryasetiawan F and Gunnarsson O 1995 *Phys. Rev. Lett.* **74** 3221
- [56] Chevreau H, Moreira I de P R, Silvi B and Illas F 2001 *J. Phys. Chem. A* **105** 3570
- [57] Towler M D, Allan N L, Harrison N M, Saunders V R, Mackrodt C W and Aprà E 1994 *Phys. Rev. B* **50** 5041
- [58] Ricart J M, Dovesi R, Roetti C and Saunders V R 1995 *Phys. Rev. B* **52** 2381
see also Ricart J M, Dovesi R, Roetti C and Saunders V R 1997 *Phys. Rev. B* **55** 15942 (erratum)
- [59] Reinhardt P, Moreira I de P R, de Graaf C, Illas F and Dovesi R 2000 *Chem. Phys. Lett.* **319** 625
- [60] Dovesi R, Roetti C, Freyria-Fava C, Prencipe M and Saunders V R 1991 *Chem. Phys.* **156** 11
- [61] Catti M, Dovesi R, Pavese A and Saunders V R 1991 *J. Phys.: Condens. Matter* **3** 4151
- [62] Su Y-S, Kaplan T A, Mahanti S D and Harrison J F 2000 *Phys. Rev. B* **61** 1324
- [63] Nicastro M and Patterson C H 2002 *Phys. Rev. B* **65** 205111
- [64] Fulde P 2002 *Adv. Phys.* **51** 909
- [65] Fink K and Staemmler V 1995 *J. Chem. Phys.* **103** 2603
- [66] Shukla A, Dolg M, Fulde P and Stoll H 1999 *Phys. Rev. B* **60** 5211
- [67] Colle R and Salvetti O 1975 *Theor. Chim. Acta* **37** 329
Colle R and Salvetti O 1979 *Theor. Chim. Acta* **53** 55
- [68] Colle R and Salvetti O 1993 *J. Chem. Phys.* **79** 1404
- [69] Becke A D 1993 *J. Chem. Phys.* **99** 1372
- [70] Becke A D 1993 *J. Chem. Phys.* **98** 5648
- [71] Becke A D 1996 *J. Chem. Phys.* **104** 1040
- [72] Lee C, Yang W and Parr R G 1988 *Phys. Rev. B* **37** 785
- [73] Muscat J, Wander A and Harrison N M 2001 *Chem. Phys. Lett.* **342** 397
- [74] Bredow T and Gerson A R 2000 *Phys. Rev. B* **61** 5194
- [75] Perry J K, Tahir-Kheli J and Goddard W A 2001 *Phys. Rev. B* **63** 4510
- [76] Moreira I de P R, Illas F and Martin R L 2002 *Phys. Rev. B* **65** 155102
- [77] Martin R L and Illas F 1997 *Phys. Rev. Lett.* **79** 1539
- [78] Markovits A, Skalli M K, Minot C, Pacchioni G, López N and Illas F 2001 *J. Chem. Phys.* **115** 8172
- [79] López N, Paniagua J C and Illas F 2002 *J. Chem. Phys.* **117** 9445
- [80] de Graaf C, Illas F, Broer R and Nieuwpoort W C 1997 *J. Chem. Phys.* **106** 3287
- [81] de Graaf C, Broer R and Nieuwpoort W C 1997 *Chem. Phys. Lett.* **271** 372
- [82] Pacchioni G and Illas F 2003 *Catalysis and Electrocatalysis at Nanoparticle Surfaces* ed A Wieckowski, E Savinova and C G Vayenas (New York: Dekker) p 65
- [83] Winter N W, Pitzer R M and Temple D K 1987 *J. Chem. Phys.* **86** 3549
- [84] Winter N W and Pitzer R M 1988 *J. Chem. Phys.* **89** 446
- [85] Barandiarán Z and Seijo L 1988 *J. Chem. Phys.* **89** 5739
- [86] Seijo L and Barandiarán Z 1999 *Computational Chemistry: Reviews of Current Trends* (Singapore: World Scientific)
- [87] Evjen H M 1932 *Phys. Rev.* **39** 675
- [88] Sousa C, Casanovas J, Rubio J and Illas F 1993 *J. Comput. Chem.* **14** 680
- [89] Reinhardt P, Habas M P, Dovesi R, Moreira I de P R and Illas F 1999 *Phys. Rev. B* **59** 1016
- [90] Barandiarán Z and Seijo L 1992 *Cluster Models for Surface and Bulk Phenomena* ed G Pacchioni, P S Bagus and F Parmigiani (New York: Plenum) p 565
- [91] Pisani C and Birkenheuer U 1996 *Comput. Phys. Commun.* **96** 152
- [92] Pisani C, Corà F, Nada R and Orlando R 1994 *Comput. Phys. Commun.* **82** 139
- [93] Born M 1920 *Z. Phys.* **1** 45
- [94] Dick B G and Overhauser A W 1958 *Phys. Rev.* **112** 90
- [95] Catlow C R A, Dixon M and Mackrodt W C 1982 *Computer Simulation of Solids* ed C R Catlow (Berlin: Springer) p 130

- [96] Pisani C, Dovesi R and Roetti C 1988 *Hartree-Fock ab initio Treatment of Crystalline Systems (Springer Lecture Notes in Chemistry vol 48)* (Heidelberg: Springer)
- [97] Saunders V R, Dovesi R, Roetti C, Causà M, Harrison N M, Orlando R and Zicovich-Wilson C M 1998 *CRYSTAL98 User's Manual* (Torino: University of Torino)
- [98] Blaha P, Schwarz K and Luitz J 1999 *WIEN97, A Full Potential Linearized Augmented Plane Wave Package for Calculating Crystal Properties* Technical University of Vienna (ISBN 3-9501031-0-4)
This is an improved and updated Unix version of the original copyrighted WIEN code, which was published by
Blaha P, Schwarz K, Surantin P and Trickey S B 1990 *Comput. Phys. Commun.* **59** 399
- [99] Kresse G and Hafner J 1993 *Phys. Rev. B* **47** 558
- [100] Kresse G and Furthmüller J 1996 *Comput. Mater. Sci.* **6** 15
- [101] Kresse G and Furthmüller J 1996 *Phys. Rev. B* **54** 11169
- [102] <http://www.fysik.dtu.dk/CAMPOS/WhatIs/dacapo.html>
- [103] Roos B O, Taylor P and Siegbahn P 1980 *Chem. Phys.* **48** 157
- [104] Siegbahn P, Heiberg A, Roos B O and Levy B O 1980 *Phys. Scr.* **21** 323
- [105] User's manual for MOLCAS 4.0 program
- [106] Andersson K, Malmqvist P-Å, Roos B O, Sadlej A J and Wolinski K 1990 *J. Phys. Chem.* **94** 5483
- [107] Andersson K, Malmqvist P-Å and Roos B O 1992 *J. Chem. Phys.* **96** 1218
- [108] Hay P J and Wadt W R 1985 *J. Chem. Phys.* **82** 299
- [109] Widmark P-O, Malmqvist P-Å and Roos B O 1990 *Theor. Chim. Acta* **77** 291
- [110] Widmark P-O, Persson B J and Roos B O 1991 *Theor. Chim. Acta* **79** 419
- [111] Pierloot K, Dumez B, Widmark P-O and Roos B O 1995 *Theor. Chim. Acta* **90** 87
- [112] Pou-Amérgo R, Merchán M, Nebot-Gil I, Widmark P-O and Roos B O 1995 *Theor. Chim. Acta* **92** 149
- [113] Vanderbilt D H 1990 *Phys. Rev. B* **41** 7892
- [114] de Graaf C, Sousa C, Moreira I de P R and Illas F 2001 *J. Phys. Chem. A* **105** 11371
- [115] Moore C E 1971 *Tables of Atomic Energy Levels* NBS Circular (Washington, DC: US Government Printing Office)
see also information on <http://physlab2.nist.gov/PhysRefData/contents.html>
- [116] Andersson K and Roos B O 1992 *Chem. Phys. Lett.* **191** 507
- [117] Bauschlicher C W, Siegbahn P E M and Pettersson L G M 1988 *Theor. Chim. Acta* **74** 479
- [118] Moroni E G, Kresse G, Hafner J and Furthmüller J 1997 *Phys. Rev. B* **56** 15629
- [119] Ferrari A M and Pacchioni G 1996 *J. Phys. Chem.* **100** 9032
- [120] Matveev A V, Neyman K M, Yudanov I V and Rösch N 1999 *Surf. Sci.* **426** 123
- [121] Giordano L, Goniakowski J and Pacchioni G 2001 *Phys. Rev. B* **64** 75417
- [122] López N and Illas F 1998 *J. Phys. Chem. B* **102** 1430
- [123] López N, Illas F, Rösch N and Pacchioni G 1999 *J. Chem. Phys.* **110** 4873
- [124] Hammer B, Hansen L B and Nørskov J 1999 *Phys. Rev. B* **59** 7413
- [125] Casanovas J, Rubio J and Illas F 1996 *Phys. Rev. B* **53** 945
- [126] Illas F, Moreira I de P R, de Graaf C, Castell O and Casanovas J 1997 *Phys. Rev. B* **56** 5069
- [127] Calzado C J, Sanz J F, Malrieu J P and Illas F 1999 *Chem. Phys. Lett.* **307** 102
- [128] Muñoz D, Illas F and Moreira I de P R 2000 *Phys. Rev. Lett.* **84** 1579
- [129] Moreira I de P R, Muñoz D, Illas F, de Graaf C and Garcia-Bach M A 2001 *Chem. Phys. Lett.* **345** 183
- [130] Calzado C J and Malrieu J P 2001 *Phys. Rev. B* **63** 214520
- [131] Muñoz D, Moreira I de P R and Illas F 2002 *Phys. Rev. B* **65** 224521
- [132] Moreira I de P R, Illas F and Martin R L 2002 *Phys. Rev. B* **65** 155102
- [133] de Graaf C, Moreira I de P R, Illas F and Martin R L 1999 *Phys. Rev. B* **60** 3457
- [134] de Graaf C and Illas F 2001 *Phys. Rev. B* **63** 014404
- [135] de Graaf C, Moreira I de P R, Illas F, Iglesias O and Labarta A 2002 *Phys. Rev. B* **66** 014448
- [136] Moreira I de P R, Suaud N, Guihéry N, Malrieu J P, Caballol R, Bofill J M and Illas F 2002 *Phys. Rev. B* **66** 134430
- [137] Moreira I de P R, Illas F, Calzado C J, Sanz J F, Malrieu J P, Ben Amor N and Maynau D 1999 *Phys. Rev. B* **59** R6593
- [138] Miralles J, Castell O, Caballol R and Malrieu J P 1993 *Chem. Phys.* **172** 33
- [139] Miralles J, Daudey J P and Caballol R 1992 *Chem. Phys. Lett.* **198** 555
- [140] Noguera C and Mackrodt W C 2000 *J. Phys.: Condens. Matter* **12** 2163
- [141] Casassa S, Ferrari A M, Busso M and Pisani C 2002 *J. Phys. Chem. B* **106** 12978
- [142] Pothuizen J J M, Cohen O and Sawatzky G A 1996 *Mater. Res. Soc. Symp. Proc.* **401** 501
- [143] Marynowski M, Franzen W, El-Batanouny M and Staemmler V 1999 *Phys. Rev. B* **60** 6053

-
- [144] El-Batanouny M 2002 *J. Phys.: Condens. Matter* **14** 6281
 - [145] Wyckoff R W G 1963 *Crystal Structures* vol 1 (New York: Wiley)
 - [146] Staemmler V and Fink K 2002 *Chem. Phys.* **278** 79
 - [147] Hutchings M T and Samuelsen E J 1972 *Phys. Rev. B* **6** 3447
 - [148] Shanker R and Singh R A 1973 *Phys. Rev. B* **7** 5000
 - [149] Koghi M, Ishikawa Y and Endoh Y 1972 *Solid State Commun.* **11** 391
 - [150] Lines M E and Jones E D 1965 *Phys. Rev.* **139** A1312
 - [151] Ködderitzsch D, Hergert W, Temmerman W M, Szotek Z, Ernst A and Winter H 2002 *Phys. Rev. B* **66** 064434